Atmos. Meas. Tech. Discuss., 4, 5837–5855, 2011
www.atmos-meas-tech-discuss.net/4/5837/2011/
doi:10.5194/amtd-4-5837-2011

Atmospheric Measurement Techniques Discussions

Field inter-comparison of two high-accuracy fast-response spectroscopic sensors of carbon dioxide

B. A. Flowers, H. H. Powers, M. K. Dubey, and N. G. McDowell

Earth and Environmental Science Division, Los Alamos National Laboratory, Los Alamos, NM 87545, USA

Received: 6 September 2011 – Accepted: 7 September 2011
– Published: 15 September 2011

Correspondence to: B. A. Flowers (bflowers@lanl.gov)

Published by Copernicus Publications on behalf of the European Geosciences Union.

Abstract

Tunable diode laser absorption (TDL) and cavity ring-down spectroscopic (CRDS) sensors for atmospheric carbon dioxide were co-deployed during summer and fall of 2010 in the field at Los Alamos National Laboratory. Both sensors were characterized for accuracy and precision for ambient carbon dioxide measurements at ground level and are compared using both laboratory and atmospheric data. After a four point laboratory cross calibration, the mean $[^{12}C^{16}O_2]_{TDL} = 392.05 \pm 8.92$ ppm and $[^{12}C^{16}O_2]'_{CRDS} = 392.22 \pm 9.05$ ppm between 29 July and 16 August 2010 (mean difference = 0.04 ± 0.04 ppm). The slope of the cross-calibrated linear regression analysis between the two sensors is 1.000. The CRDS sensor is capable of measuring ambient $[^{12}C^{16}O_2]$ to a relative precision of 23 ppb $Hz^{-1/2}$ for a 1-min time constant and this decreases to 6.5 ppb $Hz^{-1/2}$ for a 58-min time constant. At one and 58-min time constants, the TDL exhibits precisions of 29 ppb $Hz^{-1/2}$ and 53 ppb $Hz^{-1/2}$. The CRDS is compact, fast, and stable. The TDL is larger and requires frequent calibrations that limit its time resolution. Field observations show that 1-min averaged data measured by the two instruments agree almost perfectly, for the 19-day period the CRDS/TDL ratio is a Gaussian distribution at $x_0 = 1.000 \pm 3.38 \times 10^{-5}$. The sensors also exhibit consistent hourly averaged diurnal values underscoring the interplay of biological, anthropogenic, and transport processes regulating CO_2 at the site.

1 Introduction

Sensors based on optical spectroscopy are important tools for rapid, accurate in situ measurements of greenhouse gases for biosphere-atmosphere flux measurements and source attribution applications. Sensors using mid-IR and IR laser sources or high finesse optical cavities are the state of the art for continuously sensing greenhouse gases with precision(s) approaching that of isotope ratio mass spectrometry for isotopic

AMTD
4, 5837–5855, 2011

analysis schemes (Powers et al., 2010; Karlon et al., 2010; Brown, 2003; Chen et al., 2010). Numerous laser-based sensors are undergoing rapid development to study greenhouse gases, thus it is important to conduct instrument inter-comparisons to establish their relative precisions under field conditions. The World Meteorological Organization/International Atomic Energy Agency recommends laboratory inter-comparison agreement of ±0.1 ppm for $^{12}C^{16}O_2$ between operational techniques and further recommends the CO_2 mixing ratios be measured for dry gases (WMO, 2005). We intercompare a commercially available cavity ring-down absorption analyzer (CRDS) with a tunable diode laser absorption (TDL) system for monitoring carbon dioxide [$^{12}C^{16}O_2$].

We conduct the study in both the laboratory and field settings to establish accuracy and precision for the two sensors. In the laboratory, the CRDS analyzer was run on the TDL analyzer's operational calibration protocol so both sensors measured the same standard gas in the laboratory. In the field, we compare the ambient carbon dioxide data sets obtained from the sensors obtained during a 19-day period in late summer 2010. For ambient measurements, the CRDS analyzer and TDL sensors were set up at the same field site and were run with their respective sampling protocol to get the best data possible from each sensor. Both the CRDS and TDL sensors are used throughout the climate and ecosystem research and environmental sensing communities and it is important to directly compare the results of laser-based optical absorption sensors operating via related principles but different technique to ensure data sets from either sensor are in agreement with references and each other. The purpose of this paper is to compare [$^{12}C^{16}O_2$] obtained operating the CRDS and TDL sensors under their optimal operational protocols.

2 Methods

The carbon dioxide sensors used in this study are a cavity ring-down analyzer (Picarro 1301-m, Picarro, Inc. CA, USA) (Crosson, 2008) and a TDL absorption sensor (TGA100, Campbell Scientific, Logan, UT). The CRDS sensor measures $^{12}C^{16}O_2$,

AMTD
4, 5837–5855, 2011

$^{12}C^{1}H_4$, and $^{1}H_2^{16}O$ while the TDL sensor measures isotopologues of CO_2: $^{12}C^{16}O_2$, $^{13}C^{16}O_2$, $^{18}O^{12}C^{16}O$ by direct absorption near 2309 cm^{-1} (Bowling et al., 2003). For direct comparison, only the $^{12}C^{16}O_2$ signals from either instrument are used in this work. Both the CRDS and TDL instruments have been described previously (e.g., Crosson et al., 2008; Bowling et al., 2003) and the TDL sensor used in this study has been described in Powers et al. (2010). Briefly, the CRDS sensor uses mid-IR diode lasers that do not require liquid nitrogen cooling, whereas the lead-salt diode in the TDL sensor does require liquid nitrogen cooling. Similarly, the CRDS sensor does not require frequent in situ absorption response calibrations, whereas they are essential for the TDL sensor. The CRDS sensor is designed to operate without in situ calibration on ambient air, particulate matter is filtered but no drying is performed. The TDL sensor is calibrated frequently, particulate matter is filtered from its sample stream and the TDL sample is dried. The sensors were housed at a semi-arid pinon-juniper (*juniperus monosperma*) woodland site at the Los Alamos National Laboratories' Environmental Research Park (Shim et al., 2011). For ambient monitoring, air was sampled approximately 5 m above ground outside a laboratory that is surrounded by the woodland for ~74 km^2.

3 Results and discussion

3.1 Laboratory cross-calibration and instrumental precision

Over 7 months before and after the study, the linearity of the CRDS response between 0 and 487 ppm [CO_2] was measured to be 0.995 (3 May 2010), 0.994 (22 July 2010), and 0.998 (11 January 2011) using a variety of carbon dioxide reference gases and dilution settings. These checks and the inter-comparison experiments described here were performed before the CRDS sensor was deployed to the Four Corners, NM region to monitor CO_2 and CH_4 emissions (in situ and with a solar Fourier Transform Spectrometer) from power-plant and oil and gas mining

AMTD
4, 5837–5855, 2011

(https://tccon-wiki.caltech.edu/Sites/Four_Corners). The reference gases used (341, 402, 487 ppm [CO_2]) were commercially available NIST-traceable standards, though only mixed to ±2 % precision (±7–8 ppm). The CRDS analyzer had been powered down and up as well as transported to different locations for the linearity checks. Linearity checks were performed by diluting the mixtures of CO_2 in air by adding varying amounts of dry N_2(g). All gases used in the linearity checks purchased dry and no response of the CRDS sensor to water vapor were performed in these checks. Nominal conditions are controlled inside the CRDS optical cavity ($P = 139.899 \pm 0.068$ Torr, $T = 45.000 \pm 0.002$ °C), leading to stable spectroscopic features largely devoid of pressure broadening effects. The response of the CRDS sensor to water vapor has been documented (Rella, 2010; Chen et al., 2010) and the procedures recommended by the manufacturer in their 2010 white paper (Rella, 2010) have been used here to produce dry mixing ratios of carbon dioxide used for the inter-comparison. For laboratory inter-comparison, the CRDS sensor was plumbed into the flow manifold that controls the automated calibration protocol for the TDL sensor. The gas input to both sensors was cycled through a high then low concentration reference gas for 30 s each, then to an unknown sample tank for 60 s. The high and low reference gases were secondary calibration standards referenced to WMO-traceable standards from NOAA-ESRL, ($[^{12}C^{16}O_2]_{high} = 541.67 \pm 0.03$ ppm and $[^{12}C^{16}O_2]_{low} = 350.34 \pm 0.01$ ppm). The TDL analyzer routinely operates using tertiary standards cross-calibrated to the high precision WMO-traceable standards, and we calibrate the CRDS response with respect to the TDL sensor. In the TDL operation protocol, the sample $[^{12}C^{16}O_2]$ is determined by linear regression between the instrumental response to the high and low reference standards and the instrument response to sample $[^{12}C^{16}O_2]$. The TDL response to the high and low reference gases are held constant, according to their measured TDL response with respect to the WMO-traceable standards, in the linear regression to determine sampled [CO_2]. The TDL is forced to measure 557.6 ± 0.1 ppm for $[^{12}C^{16}O_2]_{high}$ and 354.6 ± 0.1 ppm for $[^{12}C^{16}O_2]_{low}$ and responded to the unknown sample $[^{12}C^{16}O_2]_{unknown} = 407.835 \pm 0.091$ ppm, a percent relative

AMTD
4, 5837–5855, 2011

standard deviation (%RSD) = 0.02 %. The CRDS had been coarsely calibrated with less precise standards(±7–8 ppm uncertainties) prior to the cross-calibration and was transported to the TDL site for the experiment. The same statistics for the CRDS sensor are $[^{12}C^{16}O_2]_{high} = 547.707 \pm 0.743$ ppm, $[^{12}C^{16}O_2]_{low} = 352.829 \pm 0.076$ ppm, and $[^{12}C^{16}O_2]_{unknown} = 405.923 \pm 0.121$ ppm, respectively (CRDS %RSD = 0.1 %, 0.02 %, and 0.03 %, respectively). The $[^{12}C^{16}O_2]$ values for the laboratory cross calibration are plotted in Fig. 1 and the slope of the linear regression between the CRDS and TDL data is the 4-point CRDS calibration factor, $f_{CRDS} = 0.989 \pm 0.005$ ($r^2 = 0.999$ for the regression analysis). This cross-calibration pegs the CRDS to the same reference standards as the TDL. The $\pm 2\sigma$ standard deviations for each concentration are used as error bars, but are too small to see in the plot. The calibration factor is based on reference standards known to a higher precision (sub ppm compared with a few ppm) and wider concentration range than any used in previous checks for linearity. We use the f_{CRDS} calibration factor determined from precise tertiary standards to derive ambient concentrations: $f_{CRDS} \times [^{12}C^{16}O_2]_{CRDS} = [^{12}C^{16}O_2]'_{CRDS}$. The calibrated CRDS data is used for inter-comparison with the TDL.

We use the laboratory inter-comparison study to establish the precision and stability as a function of signal integration time for the CRDS and TDL measurement methods using the Allan variance technique (Werle et al., 1993). When the overall noise is dominated by random noise, increasing signal integration time decreases the variance (σ^2) until a time at which instrumental noise begins to dominate and the variance begins to increase. The maximum precision of each sensor is defined at the integration time where the signal variance is minimized. The transition between random and instrumental noise can be sharp (quick) or shallow (long), demonstrated in Bowling et al. (2003); Tuzson et al. (2010). We perform this analysis to compare the performance of the CRDS and TDL measuring a reference gas. We note the TDL is calibrated for 30 s each at high and low standards and measures the sample gas for 60 s. In contrast, the CRDS is not constantly re-calibrated and data is reported every ~0.75 s. This is apparent in the time scales of the Allan variance plot, where the

AMTD
4, 5837–5855, 2011

CRDS data begins at 1 s (black trace) and at 15 s for the TDL (red trace). Using 16 h of data at $[^{12}C^{16}O_2] = 405.923 \pm 0.121$ ppm, we estimate the precision of the CRDS sensor to be 29 ppb $Hz^{-1/2}$ at 30 s integration and 23 ppb $Hz^{-1/2}$ at 60 s integration time. The same statistics for the TDL at 30 and 60 s integration time are 34 ppb $Hz^{-1/2}$ and 29 ppb $Hz^{-1/2}$. At 58 min (3500 s integration time), the precision of the CRDS sensor is 6 ppb $Hz^{-1/2}$ and the same statistic for the TDL is 53 ppb $Hz^{-1/2}$. Figure 2 shows the Allan variance plot for the CRDS (black trace) and TDL (red trace) sensors taken from the laboratory data set. We clearly see the stability of the CRDS sensor does not show a sharp "V" shape exhibited in Allan variance plots for the TDL but a slower transition from the so-called white noise to drift noise regions of the Allan variance plot (Werle et al., 1993). This behavior is similarly exhibited by the quantum cascade laser absorption spectrometer (QCLAS) methane sensors described by Tuzson et al. (2010). The CRDS sensor exhibits stability at considerably longer integration times than does the TDL sensor, the minimum detection limit (6 ppb $Hz^{-1/2}$) is observed at 3500 s (58 min) signal integration time, opposed to 30 s (23 ppb $Hz^{-1/2}$) for the TDL, which corresponds to two calibration cycles in its measurement protocol. The CRDS detection limit at 58 min is in close agreement with the prototype CRDS sensor from the manufacturer (Van Pelt, 2011), and is here independently verified.

3.2 Continuous ambient carbon dioxide monitoring

Both the TDL and CRDS sensor were housed in a laboratory at the Los Alamos National Laboratory Environmental Research Park for the ambient carbon dioxide intercomparison study. The CRDS sensor was operated without in situ calibration for the 19-day study. The TDL CO_2 sensor measures $^{12}CO_2$ absorption near 2308.225 cm^{-1}, pressure and temperature in the TDL optical cavity were maintained at 15.0 Torr and 30 °C, respectively. The TDL sampling protocol calls for use of a Nafion dryer, ensuring that the sample measured by the instrument has similar partial pressure of H_2O as the calibration gases in the measurement cell. The TDL CO_2 analyzer requires frequent

AMTD
4, 5837–5855, 2011

calibration to maintain its stated precision. The sample stream was switched to both a high or low reference calibration gas for 30 s, then measured ambient [CO_2] for 1 min. The first 15 s of data at each stage of this cycle is ignored to account for flushing and sample equilibration in the TDL optical cavity (Powers et al., 2010).

Both the CRDS and TDL sensors sampled ambient air from a single tube that was run out of the building to a small tower approximately 4 m above ground outside the building at the Los Alamos Environmental Research Park. The tube was connected to a manifold and the CRDS and TDL sensors sampled from the manifold continuously at 500 ml min^{-1} and 200 ml min^{-1}, respectively. The sensors were run independently of each other, using their own operational sampling protocols. We characterize the agreement between the two sensors for quantitative CO_2 measurement at ground level by comparing their temporal relationships; the linear regression between their temporal signatures, and the calculated ratio and difference for their response to ambient CO_2 for the 19 day observation period. The 1-min temporal response of both sensors to ambient CO_2 near Los Alamos, NM is shown in Fig. 3. The $[^{12}C^{16}O_2]'_{CRDS}$ mixing ratio is shown on top, $[^{12}C^{16}O_2]_{TDL}$ is shown on the bottom of the plot. The ambient $[^{12}C^{16}O_2]$ signal varies between 378 and 440 ppm. The diurnal variation is ~60 ppm day^{-1} at ground level. Linear regression analysis between $[^{12}C^{16}O_2]'_{CRDS}$ and $[^{12}C^{16}O_2]_{TDL}$ is shown in Fig. 4. The linear regression analysis of the 1-min averaged signal between the sensors yields $[^{12}C^{16}O_2]'_{CRDS} = 1.00 \pm 3.5 \times 10^{-5} [^{12}C^{16}O_2]_{TDL}$, with $R^2 = 0.96$ for the ambient data. The mean ratio calculated $[^{12}C^{16}O_2]'_{CRDS}/[^{12}C^{16}O_2]_{TDL}$ for the sampling period is 1.000 ± 0.005. Also shown in Fig. 4 is a histogram of the ratio $[^{12}C^{16}O_2]'_{CRDS}/[^{12}C^{16}O_2]_{TDL}$ for the 1-min data. The peak of the gaussian fit to the histogram data is centered at $x_0 = 1.003 \pm 3.28 \times 10^{-5}$. We note the importance of synchronizing the time axis for proper inter-comparison between the two sensors. For example, on 16 August 2010 there was some drifting (both forward and backward) between the clocks on CRDS and TDL analyzers. The data had to be separated into periods that exhibited linear time relationships, analyzed for correlation

AMTD
4, 5837–5855, 2011

separately, and subsequently concatenated. Originally the correlation analysis for 16 August showed $[^{12}C^{16}O_2]_{CRDS} = 0.979 \pm 0.008[^{12}C^{16}O_2]_{TDL} + (13.10 \pm 2.95)$, a y-intercept that is statistically different from zero (and indeed may be interpreted as a 13 ppm offset in $[CO_2]$). The data on 16 August was separated into AM and PM periods and time synchronized separately. This data was merged and re-analyzed to $[^{12}C^{16}O_2]_{CRDS} = 1.003 \pm 0.007[^{12}C^{16}O_2]_{TDL} + (3.67 \pm 2.6)$, which we interpret as a zero-intercept with respect to a quantitative $[^{12}C^{16}O_2]$ offset between the two sensors. Indeed we force a y-intercept $b = 0$ for in our final analysis because both sensors should respond to a sample absent of carbon dioxide with 0 ppm, similar to Tuzson et al. (2010).

3.3 Diurnal cycle of carbon dioxide

The cross-calibration and 1-min time resolution agreement between the data sets are robust factors underlying longer time averaged data to describe the diurnal pattern of the $[^{12}C^{16}O_2]$ atmospheric background signal. The hourly averaged diurnal pattern of CO_2 is an important statistic to understand local biogenic respiration/photosynthesis processes and effects transport (including anthropogenic CO_2) in the regional CO_2 background. Raw data was averaged to 1-h time constants for each hour of the day (0–23 h) for the 19-day ambient observation study to create hourly averaged diurnal $^{12}C^{16}O_2$ profiles. Table 1 shows the median diurnal $[^{12}C^{16}O_2]$ for each hour of the day between 29 July and 16 August 2010 from the CRDS (top trace) and TDL (bottom trace) sensor. Nightly increases (hours 0–6 and 20–23) in $[^{12}C^{16}O_2]$ (both in magnitude and variability) are due to respiration and daily (hours 7–19) uptake of $[^{12}C^{16}O_2]$ by photosynthesis is evident in data sets from both sensors. Ambient temperature is included in the third column. The fourth column in Table 1 shows the difference between the diurnal median $[^{12}C^{16}O_2]$ for each hour. The mean difference between the CRDS and TDL diurnal median values is much smaller (1.80 ± 1.50) than either of their variabilities (75th–25th percentile difference), 4.85 ± 2.40 and 5.17 ± 2.56 for CRDS

AMTD
4, 5837–5855, 2011

and TDL, respectively. The correlation factor (r^2) between the [$^{12}C^{16}O_2$] data sets is 0.91. Anti-correlation between median diurnal ambient temperature and median diurnal [$^{12}C^{16}O_2$] for both sensors is shown in Fig. 5. While the mechanisms controlling this interplay of respiration, photosynthesis, and dynamics are not the subject of our paper, it is clear that both sensors provide very consistent information.

An overview of the data available from both the CRDS and TDL sensors is shown in Fig. 6, shown between 29 July and 16 August 2010. The $^{12}C^{16}O_2$ signals from both sensors are the same 1-min signals used in the linear regression analysis and shown in Fig. 3. The CRDS system in this study provides robust performance for $^{12}C^{16}O_2$, $^{12}C^{1}H_4$, and $^{1}H_2^{16}O$ monitoring and is readily deployable to field sites (especially remote sites as the CRDS sensor requires no consumables for extended periods) and mobile platforms including aircraft. There is no isotopic speciation data available from this particular CRDS sensor, however it does measure CH_4 and a new version of the sensor includes CO measurement. The TDL system used here is designed to determine $\delta^{13}C$ and $\delta^{18}O$ ratios in CO_2 at stationary sites. The TDL is capable of measuring 99.91 % of the naturally occurring gaseous CO_2 isotopes and monitoring the $\delta^{13}C$ and $\delta^{18}O$ ratios in CO_2 as tracers of air mass history and soil-atmosphere exchange (Pataki et al., 2006; Shim et al., 2011; Powers et al., 2010). However, it is large and requires liquid N_2 cooling and regular calibration making it less ideal for mobile applications.

4 Conclusions

We report the results of a field and laboratory inter-comparison experiment between two commercially available spectroscopic carbon dioxide ($^{12}C^{16}O_2$) sensors. Over a 19-day period after cross calibration the agreement between the two sensors was perfect (1.000) for fast response (1 min) measurements to ambient carbon dioxide ($^{12}C^{16}O_2$). Both sensors were observed to behave linearly over a range of ambient [CO_2] (380–450 ppm) and in laboratory (354–557 ppm). The robust agreement

AMTD
4, 5837–5855, 2011

between these sensors underscores their fast, quantitative [$^{12}C^{16}O_2$] capability for atmosphere-biosphere exchange and ambient carbon dioxide (ground, mobile, and flight) measurements. For 1-min data, the mean difference between $[^{12}C^{16}CO_2]'_{CRDS}$ and $[^{12}C^{16}O_2]_{TDL}$ was 0.04 ± 0.4 ppm for dry gas [$^{12}C^{16}O_2$] measurement over the 19-day period, hence we demonstrate that the CRDS and TDL instruments are in agreement with the WMO/IAEA recommendation of ±0.100 ppm for dry [$^{12}C^{16}O_2$], once they are cross-calibrated. Operational in situ calibration of the CRDS system is needed infrequently (especially for ground based sensing), but periodic calibration with high precision standards should be performed to ensure linearity of its response under ambient [CO_2] conditions. Over 12 months of operation, we have not observed non-linear behavior for either the CRDS or TDL sensors in a wide variety of applications. Both sensors provide valuable data for carbon dioxide monitoring and their additional data streams put the $^{12}C^{16}O_2$ data stream in different contexts. Inter-comparison for isotopic speciation sensors (e.g., $^{13}C^{16}O_2$ and $^{18}O^{12}C^{16}O$) should be investigated for appropriate sensors to compare their performance. Our study will be especially valuable for analysis of experiments where multiple high precision fast response instruments are measuring greenhouse gases and differences may need to be interpreted and diagnosed (Wofsy, 2011).

Acknowledgements. BAF and MKD acknowledge the US Department of Energy ASR program and LANL's Laboratory Directed Research and Development program (LDRD). HP and NM acknowledge Clif Meyer, LANL's LDRD program and the Institute for Geophysical and Planetary Physics (IGPP) Programs.

References

Bowling, K., Sargent, S. D., Tanner, B. D., and Ehleringer, J. R.: Tunable diode laser absorption spectroscopy for stable isotope studies of ecosystem-atmosphere CO_2 exchange, Agric. Forest Meteorol., 118, 1–19, 2003.

AMTD
4, 5837–5855, 2011

Brown, S. S.: Absorption Spectroscopy in High-Finesse Cavities for Atmospheric Studies, Chemical Reviews, 103, 5219–5238, doi:10.1021/cr020645c, 2003.
Chen, H., Winderlich, J., Gerbig, C., Hoefer, A., Rella, C. W., Crosson, E. R., Van Pelt, A. D., Steinbach, J., Kolle, O., Beck, V., Daube, B. C., Gottlieb, E. W., Chow, V. Y., Santoni, G. W., and Wofsy, S. C.: High-accuracy continuous airborne measurements of greenhouse gases (CO_2 and CH_4) using the cavity ring-down spectroscopy (CRDS) technique, Atmos. Meas. Tech., 3, 375–386, doi:10.5194/amt-3-375-2010, 2010.
Crosson, E. R.: A cavity ring-down analyzer for measuring atmospheric levels of methane, carbon dioxide, and water vapor, Appl. Physics B, 92, 403–408, 2008.
Karlon, A., Sweeney, C., Tans, P., and Newberger, T.: AirCore: An Innovative Atmospheric Sampling System, J. Atmospheric Oceanic Technol., 27, 1839–1852, 2010.
Pataki, D. E., Bowling, D. R., Ehleringer, J. R., and Zobitz, J. M.: High resolution atmospheric monitoring of urban carbon dioxide sources, Geophys. Res. Lett., 33, L03813, doi:10.1029/2005GL024822, 2006.
Powers, H. H., Hunt, J. E., Hanson, D. T., and McDowell, N. G.: A dynamic soil chamber system coupled with a tunable diode laser for online measurements of $\delta^{13}C$, $\delta^{18}O$, and efflux rate of soil-respired CO_2, Rapid Communications in Mass Spectrometry, 24, 243–253, 2010.
Rella, C.: Accurate Greenhouse Gas Measurements in Humid Gas Streams Using the Picarro G1301 Carbon Dioxide/Methane/Water Vapor Gas Analyzer, Sunnyvale, CA, 2010.
Shim, J., Powers, H. H., Meyer, C., Pockman, W., and McDowell, N.: The role of inter-annual, seasonal, and synoptic climate on the carbon isotope ratio of ecosystem respiration at a semi-arid woodland, Global Change Biology, 8, 2584–2600, 2011.
Tuzson, B., Hiller, R. V., Zeyer, K., Eugster, W., Neftel, A., Ammann, C., and Emmenegger, L.: Field intercomparison of two optical analyzers for CH_4 eddy covariance flux measurements, Atmos. Meas. Tech., 3, 1519–1531, doi:10.5194/amt-3-1519-2010, 2010.
Werle, P., Mücke, R., and Slemr, F.: The Limits of Signal Averaging in Atmospheric Trace-Gas Monitoring by Tunable Diodle-Laser Absorption Spectroscopy (TDLAS), Appl. Physics B, 57, 131–139, 1993.
WMO: 13th WMO/IAEA Meeting of Experts on Carbon Dioxide Concentration and Related Tracers Measurement Techniques, World Metereological Organization, Boulder, CO, 2005.
Wofsy, S. C.: HIAPER Pole-to-Pole Observations (HIPPO): fine-grained, global-scale measurements of climatically important atmospheric gases and aerosols, Phil. Trans. Roy. Soc. A, 369, 2073–2086, 2011.

AMTD
4, 5837–5855, 2011

Table 1. Hourly diurnal median $[CO_2]'_{CRDS}$, $[CO_2]_{TDL}$, ambient temperature (°C), and the absolute value of $\Delta[CO_2]$ (CRDS – TDL) measured between 29 July and 16 August 2010 near Los Alamos, NM.

Hour	$[CO_2]'_{CRDS}$	$[CO_2]_{TDL}$	Temp. (°C)	$\Delta[CO_2]$
0	398.20	399.41	19.6	1.21
1	399.50	400.98	18.3	1.30
2	400.15	401.18	18.0	1.02
3	401.28	402.30	17.7	1.02
4	402.54	401.53	17.3	1.01
5	401.77	403.41	17.0	1.64
6	404.10	398.86	16.3	5.23
7	399.10	393.67	17.0	5.41
8	393.37	390.47	17.7	2.90
9	391.07	388.55	19.0	2.52
10	388.97	386.19	21.0	2.78
11	386.35	384.21	22.3	2.14
12	384.35	382.59	23.7	1.75
13	382.67	382.89	25.0	0.22
14	382.66	381.94	25.3	0.72
15	381.97	381.75	25.7	0.22
16	382.13	381.96	26.0	0.17
17	382.28	383.62	25.7	1.34
18	383.23	386.25	25.7	3.02
19	391.12	389.83	23.5	3.71
20	391.23	393.85	22.3	2.62
21	394.66	394.06	21.0	0.60
22	394.34	393.83	21.0	0.51
23	394.13	394.04	20.0	0.09
Mean	391.55 ± 7.52	391.92 ± 7.66		1.80 ± 1.50

AMTD
4, 5837–5855, 2011

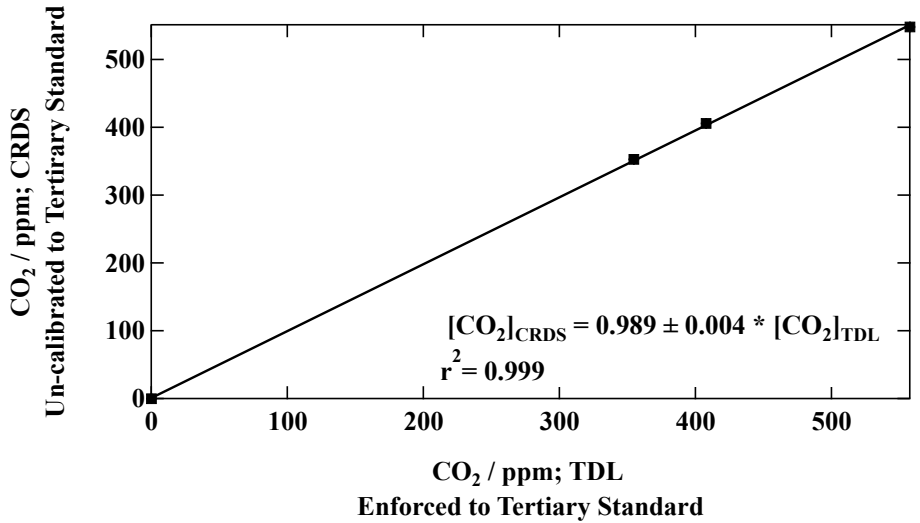

Fig. 1. Four point calibration plot of CRDS sensor with TDL tertiary standards showing linear range of calibration between 375 and 560 ppm CO_2.

AMTD
4, 5837–5855, 2011

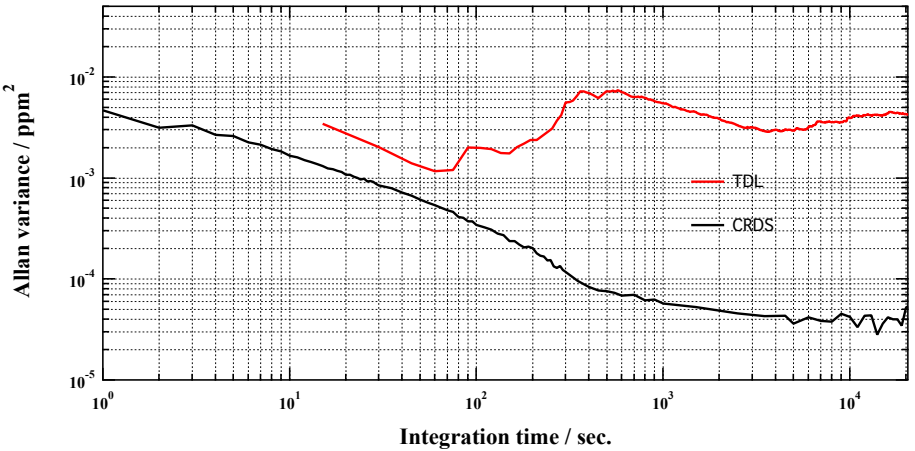

Fig. 2. Allan variance plot for CRDS sensor (black trace) and TDL (red trace) for 16 h of data shown as a log-log plot of signal variance vs. signal integration time. The minimum variance is observed at 58-min signal integration time for the CRDS sensor and at 60 s for the TDL sensor.

AMTD
4, 5837–5855, 2011

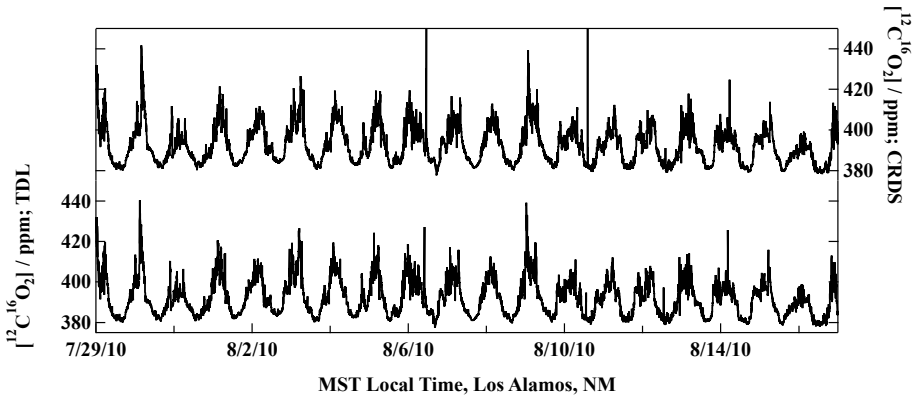

Fig. 3. Temporal profile of [$^{12}C^{16}O_2$] mixing ratio measured near Los Alamos, NM with CRDS and TDL sensors. The CRDS signal has been cross-calibrated, as described in the text.

AMTD
4, 5837–5855, 2011

High-accuracy fast-response spectroscopic sensors of CO_2

B. A. Flowers et al.

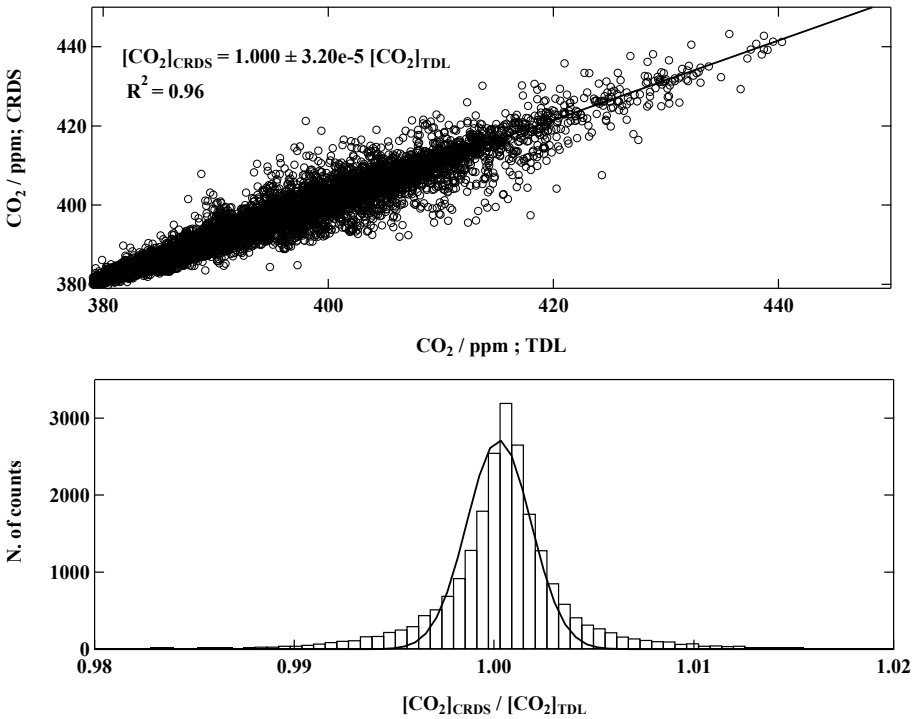

Fig. 4. Linear regression analysis of $^{12}C^{16}O_2$ measured with commercial CRDS and TDL analyzers after cross calibration using 1-min time resolution. The histogram plot of the ratio between the CRDS and TDL measurements and the gaussian fit of the $[CO_2]'_{CRDS}/[CO_2]_{TDL}$ ratio is centered on an x_0 value of 1.003.

AMTD
4, 5837–5855, 2011

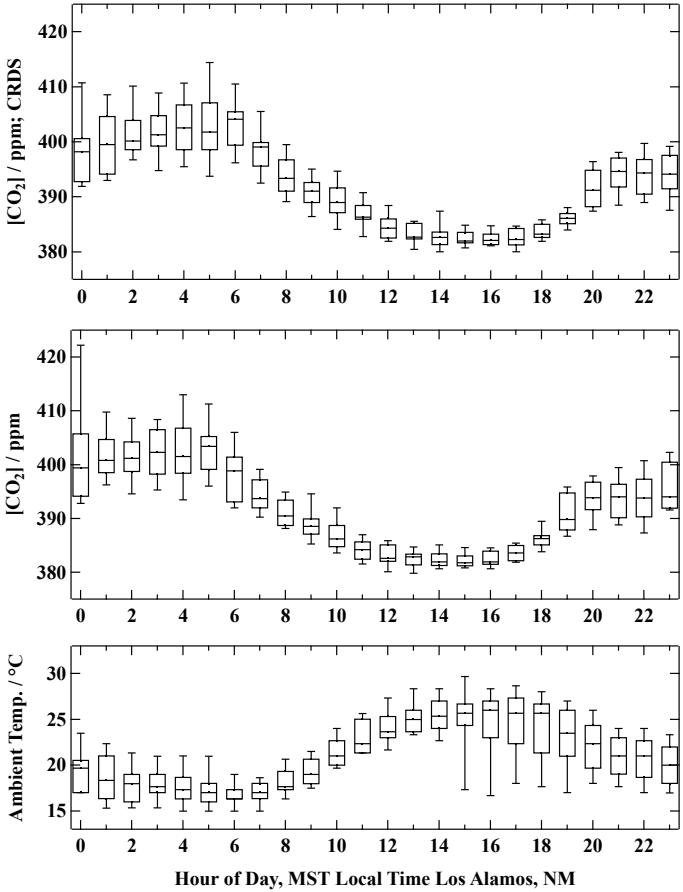

Fig. 5. Hourly diurnal median [CO_2] between 29 July and 16 August 2010 near Los Alamos NM. The scaled CRDS $[^{12}C^{16}O_2]'_{CRDS}$ trace is plotted on top, the $[^{12}C^{16}O_2]_{TDL}$ trace is plotted in the middle and hourly diurnal median ambient air temperature is plotted on the bottom trace.

AMTD
4, 5837–5855, 2011

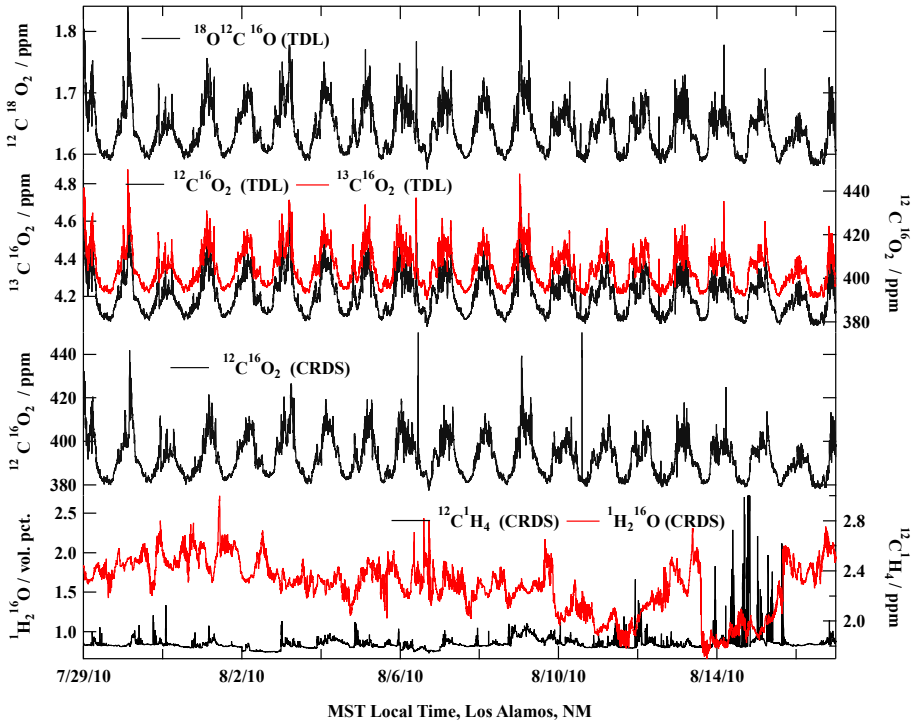

Fig. 6. One-minute traces for all signals available from both sensors used in the study. The $^{18}O^{12}C^{16}O$, $^{13}C^{16}O_2$, and $^{12}C^{16}O_2$ traces from the TDL are shown in the top of the plot while the $^{12}C^{16}O_2$, $^{12}C^{1}H_4$, and $^{1}H_2^{16}O$ traces from the CRDS are shown at the bottom. The $^{13}C^{16}O_2$ trace has been offset for clarity.

AMTD
4, 5837–5855, 2011

High-accuracy fast-response spectroscopic sensors of CO_2

B. A. Flowers et al.